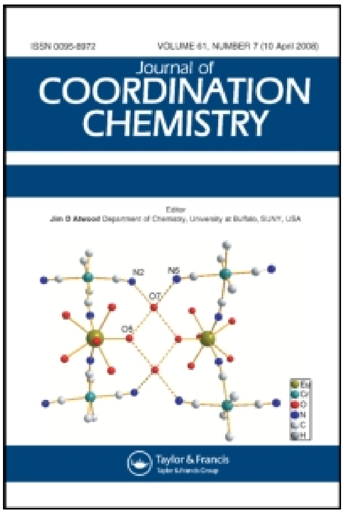

Journal of Coordination Chemistry

Publication details, including instructions for authors and subscription information:
http://www.informaworld.com/smpp/title~content=t713455674

Hydrothermal synthesis and crystal structure of two new lanthanide coordination polymers with 1,2-phenylenediacetate

Xia Li[a]; Chunyan Wang[a]; Xiangjun Zheng[b]; Yingquan Zou[b]
[a] Department of Chemistry, Capital Normal University, Beijing, China [b] Department of Chemistry, Beijing Normal University, Beijing, China

To cite this Article Li, Xia , Wang, Chunyan , Zheng, Xiangjun and Zou, Yingquan(2008) 'Hydrothermal synthesis and crystal structure of two new lanthanide coordination polymers with 1,2-phenylenediacetate', Journal of Coordination Chemistry, 61: 7, 1127 — 1136

To link to this Article: DOI: 10.1080/00958970701502003

URL: http://dx.doi.org/10.1080/00958970701502003

Journal of Coordination Chemistry
Vol. 61, No. 7, 10 April 2008, 1127–1136

Hydrothermal synthesis and crystal structure of two new lanthanide coordination polymers with 1,2-phenylenediacetate

XIA LI†, CHUNYAN WANG†, XIANGJUN ZHENG‡ and YINGQUAN ZOU*‡

†Department of Chemistry, Capital Normal University, Beijing 100037, China
‡Department of Chemistry, Beijing Normal University, Beijing 100875, China

(*Received 9 March 2007; in final form 2 July 2007*)

Two new compounds $\{[Ln_2(1,2\text{-pda})_3(H_2O)_2]\cdot 2H_2O\}_n$ (1,2-H_2pda = 1,2-phenylenediacetic acid, Ln = Tb, **1**; Ho, **2**) were prepared by hydrothermal reaction and characterized by X-ray crystallography. The Ln^{3+} is nine-coordinate by eight oxygen atoms of six 1,2-pda ligands and one oxygen of water. Ln^{3+} ions are bridged by 1,2-pda ligands *via* bridging/chelating-bridging pentadentate and chelating-bridging/chelating-bridging hexadentate coordination to form 3-D framework structures. Complex **1** emits strong green fluorescence corresponding to $^5D_4 \longrightarrow {}^7F_j$ ($j = 6$–3) transitions of the Tb^{3+}.

Keywords: Lanthanide coordination polymers; 1,2-Phenylenediacetate; Hydrothermal synthesis; Crystal structure

1. Introduction

Metal-organic coordination polymers have been studied for their interesting 1-D, 2-D, and 3-D frameworks. These complexes have potential applications in magnetism, catalysis, adsorption, and luminescent probes [1–4]. Structure and characterization of coordination polymers relate to the nature of the metal ion as nodes and the organic ligands as spacers. Lanthanide ions with large radii, high coordination numbers, special fluorescence and magnetic properties, have attracted particular attention. Polycarboxylate ligands are suitable bridging ligands because of their versatile coordination modes, and aromatic polycarboxylic acids are popular ligands in the construction of lanthanide coordination polymers with one-, two- and three-dimensional structures. For example, lanthanide coordination polymers based on benzenedicarboxylates (BDC), such as 1,2-BDC, 1,3-BDC, and 1,4-BDC, have been reported [5–10]. Phenylenediacetate (pda) is longer ($OOCCH_2$–C_6H_4–CH_2COO) than benzenedicarboxylate (OOC–C_6H_4–COO) and may lead to intriguing network structures. Few transition metal complexes with 1,3-pda and 1,4-pda have been investigated [11–14], but complexes with 1,2-pda have not been reported until now. 1,2-pda ligand is less favorable for coordination with metals compared to 1,3-pda and 1,4-pda. In this article, two new lanthanide coordination polymers

---

*Corresponding author. Tel.: +86 10 58808204. Fax: +86 10 58802075. Email: zouyq@263.net

Journal of Coordination Chemistry
ISSN 0095-8972 print/ISSN 1029-0389 online © 2008 Taylor & Francis
DOI: 10.1080/00958970701502003

with 1,2-pda, $\{[Ln_2(1,2\text{-pda})_3(H_2O)_2]\cdot 2H_2O\}_n$, have been synthesized hydrothermally; the syntheses and structural characteristics of the two complexes are reported.

2. Experimental

2.1. *Materials and methods*

$Ln(NO_3)_3\cdot 6H_2O$ (Ln=Tb, Ho) were prepared by dissolving oxides in nitric acid and then drying the solution. Elemental analysis was performed on an Elementar Vario EL analyzer. The IR spectra were recorded with a Bruker EQUINOX-55 using KBr pellets. Thermogravimetric analysis was performed on a WCT-1A thermal analyzer at a heating rate 10°C/min in air. Fluorescence spectra were measured on a F-4500 FL spectrophotometer in the solid state at room temperature.

2.2. *Synthesis of the complexes*

A mixture of 1,2-H_2pda (0.3 mmol), $Tb(NO_3)_3\cdot 6H_2O$ (0.2 mmol) or $Ho(NO_3)_3\cdot 6H_2O$ (0.2 mmol), aqueous solution of NaOH (0.3 mL, 0.5 mol L^{-1}), and deionized water (5 mL) was sealed in a Teflon-lined stainless vessel (25 mL). The vessel was heated at 160°C for 72 h and then slowly cooled to room temperature. Colorless column crystals of the title complexes were obtained. Yield, about 42%. For complex **1**, $C_{15}H_{16}O_8Tb$ (479.21), Calcd (%): C, 37.28; H, 3.36. Found (%): C, 37.09; H, 3.42. Selected IR (KBr pellet, ν/cm^{-1}): 3336 br, 1616 s, 1570 vs, 1430 s, 1415 s, 1270 s, 852 w, 727 m, 576 w, 420 w. For complex **2**, $C_{15}H_{16}O_8Ho$ (489.21), Calcd (%): C, 36.83; H, 3.30. Found (%): C, 36.58; H, 3.58. Selected IR (KBr pellet, ν/cm^{-1}): 3346 br, 1613 s, 1567 vs, 1425 vs, 1395 vs, 1270 s, 849 w, 728 m, 577 w, 419 w.

2.3. *X-ray crystallographic study*

X-ray crystal data for the complexes is collected on a Bruker Smart 1000CCD diffractometer with monochromated Mo-Kα radiation ($\lambda = 0.71073$ Å) at 293 K. Semi-empirical absorption corrections were applied using the SADABS program. All calculations were carried out on a computer with use of SHELXS-97 and SHELXL-97 programs [15, 16]. The structures were solved by direct methods and refinement on F^2 using the full-matrix least-squares methods. Summaries of the crystallographic data and details of the structure refinements are listed in table 1. Selected bond lengths and angles of **1** and **2** are listed in tables 2 and 3, respectively.

3. Results and discussion

3.1. *Structural description of complexes*

Figure 1 shows the coordination environment of Tb^{3+} in $\{[Tb_2(1,2\text{-pda})_3(H_2O)_2]\cdot 2H_2O\}_n$ (**1**). Six 1,2-pda ligands and one water surround $Tb1^{3+}$. The dihedral

Table 1. Crystallographic data for **1** and **2**.

Complex	**1**	**2**
Formula	$C_{15}H_{18}O_8Tb$	$C_{15}H_{18}O_8Ho$
Formula weight	479.18	489.21
Crystal system	Monoclinic	Monoclinic
Space group	$C2/c$	$C2/c$
Unit dimensions (Å,°)		
a	26.2699(4)	26.317(4)
b	16.0274(2)	16.004(3)
c	7.6724(1)	7.6263(12)
α	90.00	90.00
β	93.345(1)	93.471(2)
γ	90.00	90.00
V (Å)^3	3224.87(8)	3206.1(9)
Z	8	8
Calculated density (Mg m^{-3})	3.744	2.027
Absorption coefficient (mm^{-1})	4.426	4.976
$F(000)$	1848	1896
Crystal size (mm^3)	$0.32 \times 0.20 \times 0.14$	$0.06 \times 0.08 \times 0.24$
Range for data (°)	1.55 to 28.29	1.49 to 25.02
Reflections collected/unique	16210/3968 [R(int) = 0.0294]	8034/2815 [R(int) = 0.0331]
Index ranges	$-33 \geq h \geq 31$, $-21 \geq k \geq 18$, $-10 \geq l \geq 10$	$-30 \geq h \geq 31$, $-19 \geq k \geq 12$, $-9 \geq l \geq 7$
Data/restraints/parameters	3968/0/217	2815/0/217
Goodness-of-fit on F^2	1.003	1.069
Final R indices [$I > 2\sigma(I)$]	0.0254, 0.0768	0.0428, 0.1185
R indices (all data)	0.0314, 0.0804	0.0476, 0.1236

Table 2. Selected bond lengths (Å) and angles (°) for **1**.

Tb(1)–O(1)	2.422(3)	Tb(1)–O(2)#1	2.292(2)
Tb(1)–O(3)#2	2.410(3)	Tb(1)–O(3)#4	2.474(3)
Tb(1)–O(4)#4	2.504(3)	Tb(1)–O(5)	2.397(3)
Tb(1)–O(5)#3	2.462(3)	Tb(1)–O(6)	2.504(3)
Tb(1)–O(7)	2.445(3)		
O(1)–Tb(1)–O(3)#4	76.67(9)	O(1)–Tb(1)–O(4)#4	103.59(10)
O(1)–Tb(1)–O(5)#3	77.43(9)	O(1)–Tb(1)–O(6)	106.18(10)
O(1)–Tb(1)–O(7)	141.30(9)	O(2)#1–Tb(1)–O(1)	144.16(9)
O(2)#1–Tb(1)–O(5)	78.92(10)	O(2)#1–Tb(1)–O(3)#2	74.56(10)
O(2)#1–Tb(1)–O(3)#4	127.41(10)	O(2)#1–Tb(1)–O(4)#4	80.66(10)
O(2)#1–Tb(1)–O(5)#3	133.53(10)	O(2)#1–Tb(1)–O(6)	87.95(11)
O(2)#1–Tb(1)–O(7)	74.13(9)	O(3)#2–Tb(1)–O(1)	73.52(9)
O(3)#2–Tb(1)–O(3)#4	104.40(9)	O(3)#2–Tb(1)–O(4)#4	70.83(9)
O(3)#2–Tb(1)–O(5)#3	150.91(9)	O(3)#2–Tb(1)–O(6)	139.48(9)
O(3)#2–Tb(1)–O(7)	133.39(10)	O(3)#4–Tb(1)–O(4)#4	51.86(8)
O(3)#4–Tb(1)–O(6)	115.09(9)	O(4)#4–Tb(1)–O(6)	142.77(10)
O(5)–Tb(1)–O(1)	74.68(9)	O(5)–Tb(1)–O(3)#2	68.76(9)
O(5)–Tb(1)–O(3)#4	151.31(9)	O(5)–Tb(1)–O(4)#4	138.22(9)
O(5)–Tb(1)–O(5)#3	105.10(9)	O(5)–Tb(1)–O(6)	72.17(9)
O(5)–Tb(1)–O(7)	135.46(10)	O(5)#3–Tb(1)–O(3)#4	66.72(9)
O(5)#3–Tb(1)–O(4)#4	115.37(9)	O(5)#3–Tb(1)–O(6)	52.10(9)
O(7)–Tb(1)–O(3)#4	70.12(10)	O(7)–Tb(1)–O(5)#3	71.64(9)
O(7)–Tb(1)–O(4)#4	70.72(11)	O(7)–Tb(1)–O(6)	72.08(11)

Symmetry transformations used to generate equivalent atoms: #1 $x, -y+1, z-1/2$; #2 $-x+1/2, -y+3/2, -z$; #3 $x, -y+1, z+1/2$; #4 $-x+1/2, y-1/2, -z+1/2$.

Table 3. Selected bond lengths (Å) and angles (°) for **2**.

Ho(1)–O(1)#1	2.388(5)	Ho(1)–O(1)#3	2.459(5)
Ho(1)–O(2)#3	2.484(5)	Ho(1)–O(3)	2.281(5)
Ho(1)–O(4)#2	2.396(5)	Ho(1)–O(5)#2	2.487(5)
Ho(1)–O(6)	2.378(5)	Ho(1)–O(6)#2	2.439(5)
Ho(1)–O(7)	2.421(5)		
O(3)–Ho(1)–O(6)	78.48(18)	O(3)–Ho(1)–O(1)#1	74.64(18)
O(6)–Ho(1)–O(1)#1	68.58(17)	O(3)–Ho(1)–O(4)#2	144.39(16)
O(6)–Ho(1)–O(4)#2	75.08(18)	O(1)#1–Ho(1)–O(4)#2	73.74(18)
O(3)–Ho(1)–O(7)	73.90(18)	O(6)–Ho(1)–O(7)	135.35(19)
O(1)#1–Ho(1)–O(7)	133.09(19)	O(4)#2–Ho(1)–O(7)	141.31(17)
O(3)–Ho(1)–O(6)#2	133.45(18)	O(6)–Ho(1)–O(6)#2	105.39(17)
O(1)#1–Ho(1)–O(6)#2	150.90(18)	O(4)#2–Ho(1)–O(6)#2	7.20(18)
O(7)–Ho(1)–O(6)#2	71.96(19)	O(3)–Ho(1)–O(1)#3	127.80(17)
O(6)–Ho(1)–O(1)#3	151.39(18)	O(1)#1–Ho(1)–O(1)#3	104.53(17)
O(4)#2–Ho(1)–O(1)#3	76.35(18)	O(7)–Ho(1)–O(1)#3	70.30(18)
O(6)#2–Ho(1)–O(1)#3	66.48(17)	O(3)–Ho(1)–O(2)#3	80.57(19)
O(6)–Ho(1)–O(2)#3	137.69(17)	O(1)#1–Ho(1)–O(2)#3	70.59(17)
O(4)#2–Ho(1)–O(2)#3	103.71(19)	O(7)–Ho(1)–O(2)#3	70.6(2)
O(6)#2–Ho(1)–O(2)#3	115.68(16)	O(1)#3–Ho(1)–O(2)#3	52.43(16)
O(3)–Ho(1)–O(5)#2	87.3(2)	O(6)–Ho(1)–O(5)#2	72.11(17)
O(1)#1–Ho(1)–O(5)#2	139.17(17)	O(4)#2–Ho(1)–O(5)#2	106.5(2)
O(7)–Ho(1)–O(5)#2	72.2(2)	O(6)#2– Ho(1)–O(5)#2	52.60(17)
O(1)#3–Ho(1)–O(5)#2	115.32(17)	O(2)#3–Ho(1)–O(5)#2	142.8(2)

Symmetry transformations used to generate equivalent atoms: #1 $-x+1/2$, $-y+1/2$, $-z+2$; #2 $-x+1/2$, $y-1/2$, $-z+3/2$; #3 x, $-y+1$, $z-1/2$.

angles between benzene rings of the six 1,2-pda ligands are small. For example, the dihedral angles between benzene rings 1 and 2, 3 and 4, 5 and 6 (figure 1) are 0.8, 0.3, and 0.0°, respectively, which indicates all benzene rings of the six 1,2-pda ligands are coplanar or parallel and can lead to π–π stacking interactions. The $Tb1^{3+}$ is nine coordinate with eight oxygen atoms of six 1,2-pda ligands and one oxygen of water in a distorted monocapped square antiprism (figure 2). Atoms O2A, O3D, O3A and O7 and O1, O5, O5A and O6 form the upper and lower squares with mean deviations of 0.0312 and 0.0139 Å, respectively, and the dihedral angle between them is 11.1°. Atom O4A caps the upper plane. The Tb1–O(carboxylate) bond lengths vary from 2.292(2) to 2.504(3) Å with average of 2.433 Å; the Tb1–O7(water) distance is 2.445(3) Å. All 1,2-pda ligands have two coordination modes, bridging/chelating-bridging pentadentate (scheme 1a) and chelating-bridging/chelating-bridging hexadentate (scheme 1b). OCO groups of 1,2-pda ligands link adjacent Tb^{3+} ions to form a one-dimensional infinite polymeric chain (figure 3). For example, an O1C1O2 group bridges and O3AC10BO4A and O5AC11O6 groups chelate-bridge adjacent Tb^{3+} ions, Tb1 and Tb1A, with distance of 4.019 Å. These one-dimensional chains, which may be viewed as supramolecular building blocks, are further connected through 1,2-pda ligands *via* pentadentate and hexadentate coordination modes to form a 3-D network structure. If viewed along b, quadrilateral channels appear alternately. These quadrilateral channels with dimensions of 4.019 × 9.381 Å based on the Tb ⋯ b distance are formed by neighboring chains cross-linking *via* the $OOCCH_2$–C_6H_4–CH_2COO spacers of 1,2-pda ligands (figure 4). From figure 5, we can see that there are two types of channels along the *c*-axis (figures 5a and b). The B channels are formed by two 1,2-pda ligands

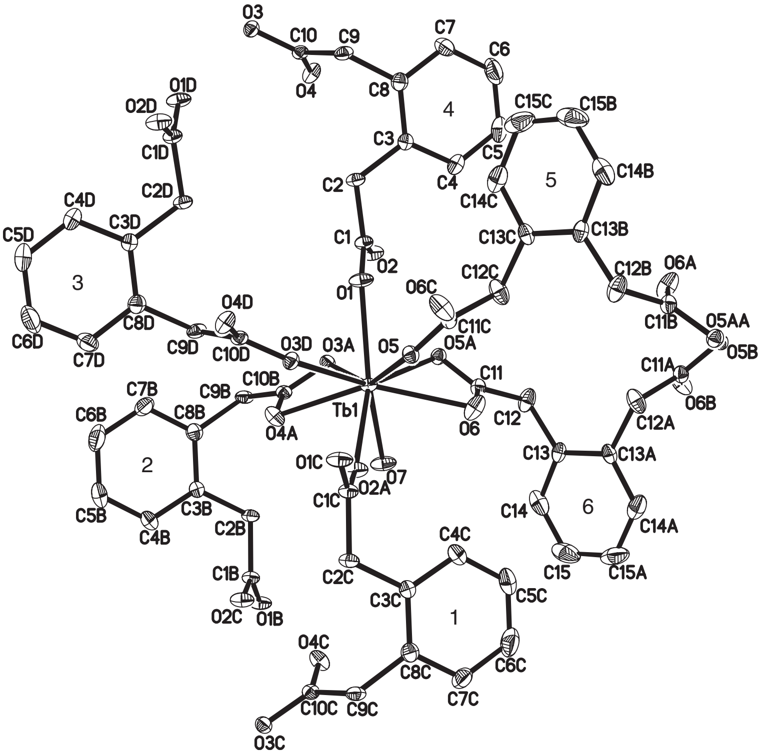

Figure 1. Coordination environment of Tb^{3+} ion in **1** at the 30% probability displacement ellipsoids. All hydrogen atoms and uncoordinated water are omitted for clarity.

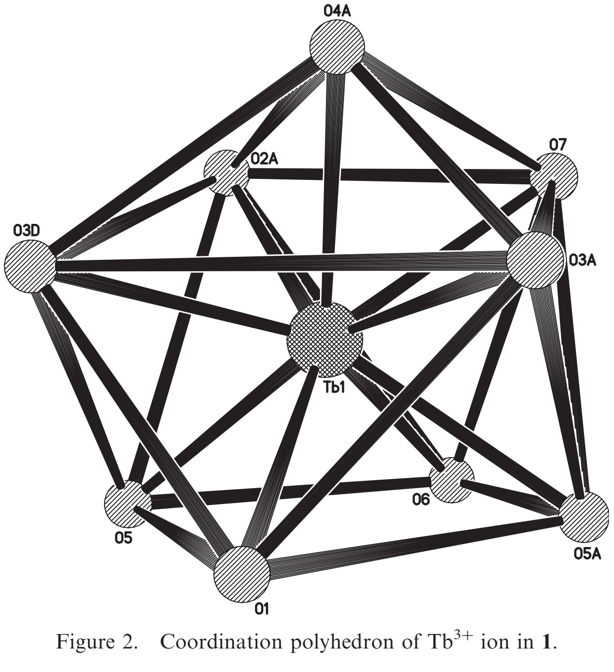

Figure 2. Coordination polyhedron of Tb^{3+} ion in **1**.

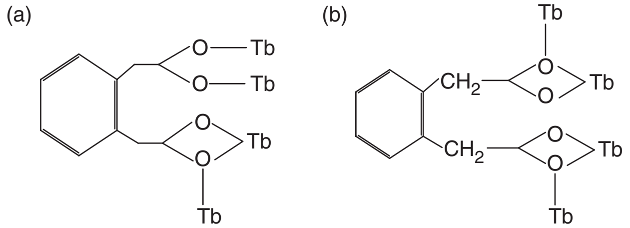

Scheme 1. Coordination modes of 1,2-pda ligands.

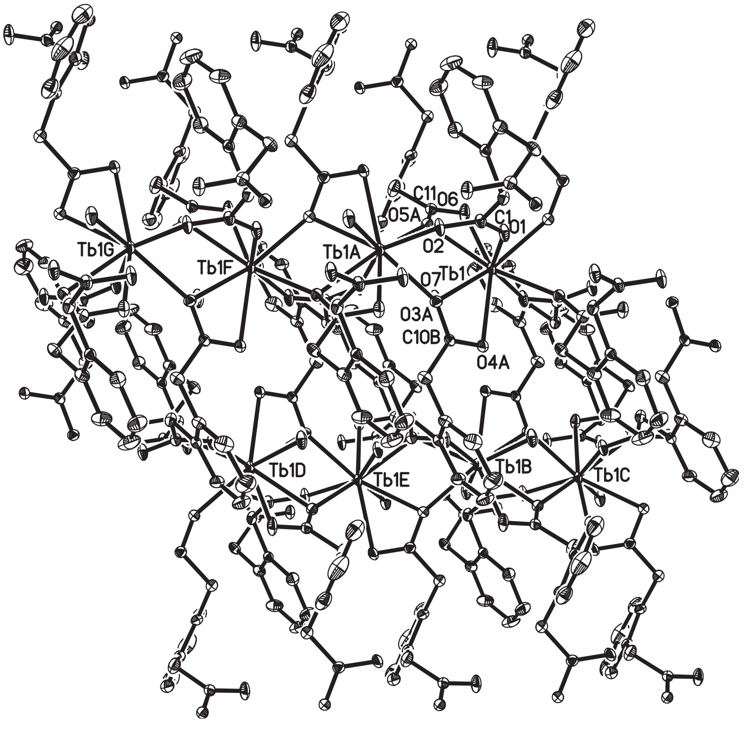

Figure 3. Chain-like structure of **1** viewed along the *a*-axis. All hydrogen atoms and uncoordinated water molecules are omitted for clarity.

and two Tb^{3+} ions, $Tb_2(1,2\text{–}OOCCH_2\text{–}C_6H_4\text{–}CH_2COO)_2$, two $OOCCH_2\text{–}C_6H_4\text{–}CH_2COO$ spacers bridge two opposite Tb^{3+} ions in 18-membered ring (2×9) channels and the distance of two opposite Tb^{3+} ions is about 9.381 Å. The six 1,2-pda ligands surrounding each Tb^{3+} simultaneously link three other Tb^{3+} ions *via* pentadentate and hexadentate coordination modes to form three 18-membered rings (figure 5b). Thus, the B channels are formed. The A channel is surrounded by six B, as shown in figure 5b. Channel A consists of six 1,2-pda ligands and six Tb^{3+} ions, $Tb_6(1,2\text{-}OOCCH_2\text{–}C_6H_4\text{–}CH_2COO)_6$, with six $OOCCH_2\text{–}C_6H_4\text{–}CH_2COO$ spacers bridging six Tb^{3+} ions to form 54-membered rings (6×9). Tb_6 units are almost coplanar with a mean deviation from

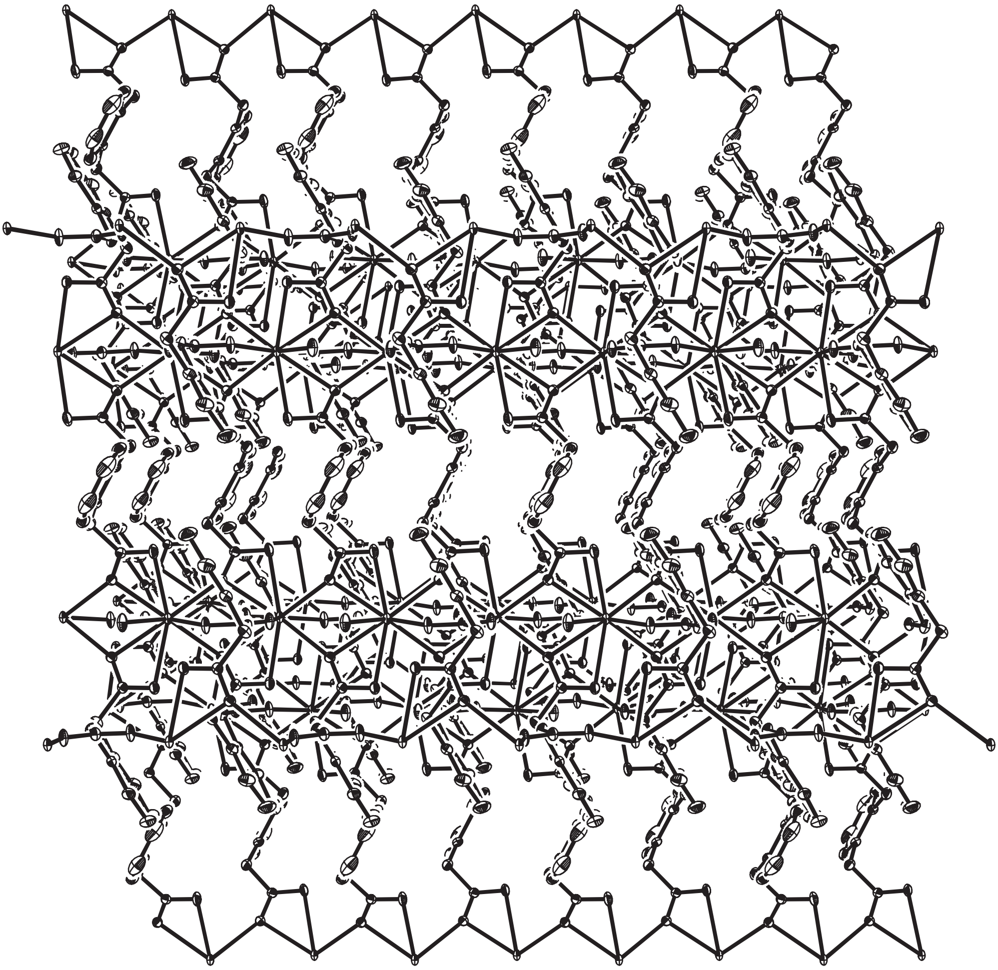

Figure 4. Packing diagram of **1** viewed along the b-axis. All hydrogen atoms and uncoordinated water are omitted for clarity.

the plane of 0.2546 Å. Ring size of channel A is 6 × 9.381 Å based on the six Tb⋯Ib separation distance. Benzene rings of 1,2-pda ligands lie in the channels. In addition, π–π stacking interactions exist between parallel benzene rings with a face-to-face distance of 3.6 Å, stabilizing the crystal structure.

Figure 6 shows the coordination environment of Ho^{3+} in $\{[Ho_2(1,2\text{-pda})_3(H_2O)_2]\cdot 2H_2O\}_n$ (**2**). Complex **2** is isomorphous with **1**. The coordination environment of Ho^{3+} in **2** is similar to that of Tb^{3+} in **1** and the structural characteristics of **2** are as described for **1**. The Ho1-O(carboxylate) bond distances are in the range 2.281(5)–2.487(5) Å with an average distance of 2.414 Å. The Ho1–O7(water) bond distance is 2.421(5) Å. The distance between two adjacent Ho^{3+} ions is 3.994(5) Å. Comparing complex **2** with **1**, obviously, d(Ho1–O (carboxylate)) < d(Tb1–O(carboxylate)), d(Ho1-O(water)) < d(Tb1–O(water)), and d(Ho1⋯Ho1) < d(Tb1⋯Tb1), related to the radius of Ho^{3+} ion being less than that of the Tb^{3+} ion, and derives from the lanthanide contraction.

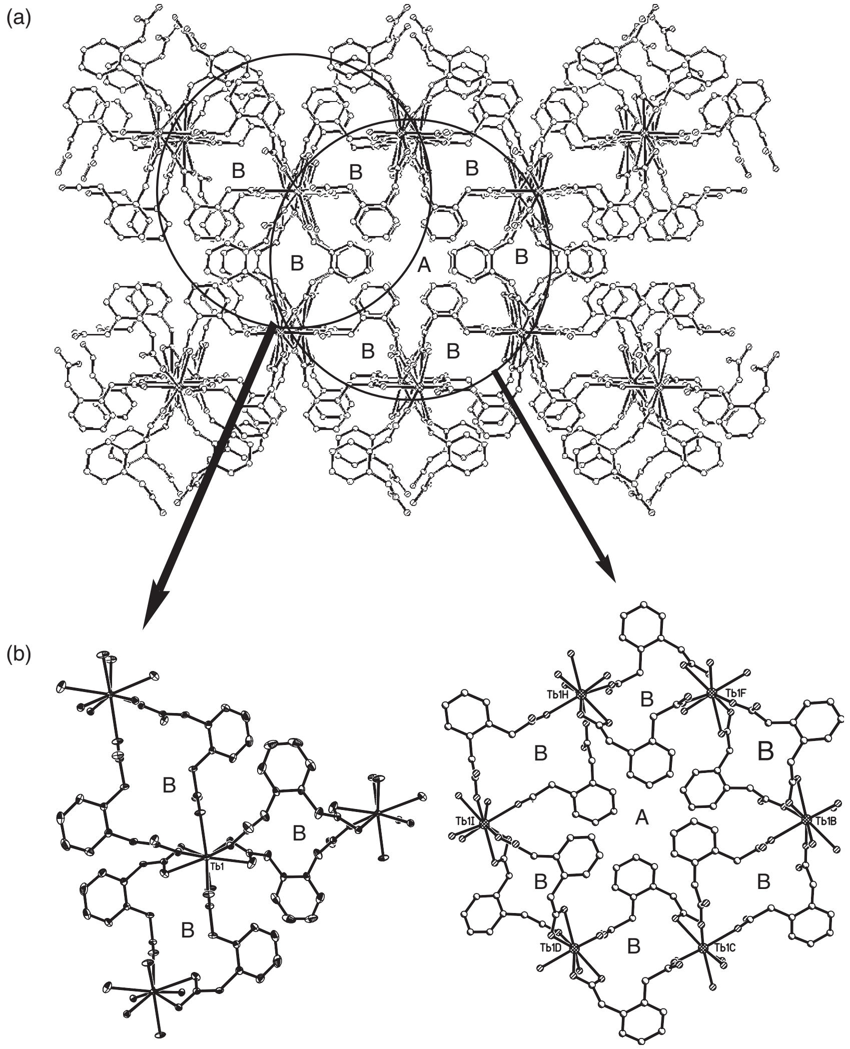

Figure 5. Packing diagram of **1** viewed along the *c*-axis. All hydrogen atoms and uncoordinated water are omitted for clarity.

3.2. *Thermogravimetric analysis*

Thermal behavior of the two complexes was studied in the temperature range 25–1000°C. For **1**, the TG curve shows that the first weight loss of 7.45% at 172°C corresponds to the loss of all free and coordination water (Calcd 7.96%). Between 403–467°C two weight losses took place. The whole weight loss of 61.82% indicates the final residue to be Tb_4O_7 (Calcd 61.32%). For **2**, the first weight loss of 3.39% at 172°C corresponds to the loss of lattice water molecule and the second weight loss of 3.39% at 263°C corresponds to the loss of the coordinated water molecule. The further decomposition between 359–398°C results in the final residue of Ho_2O_3. The total weight loss of 60.65% is in good agreement with the calculated value of 61.38%.

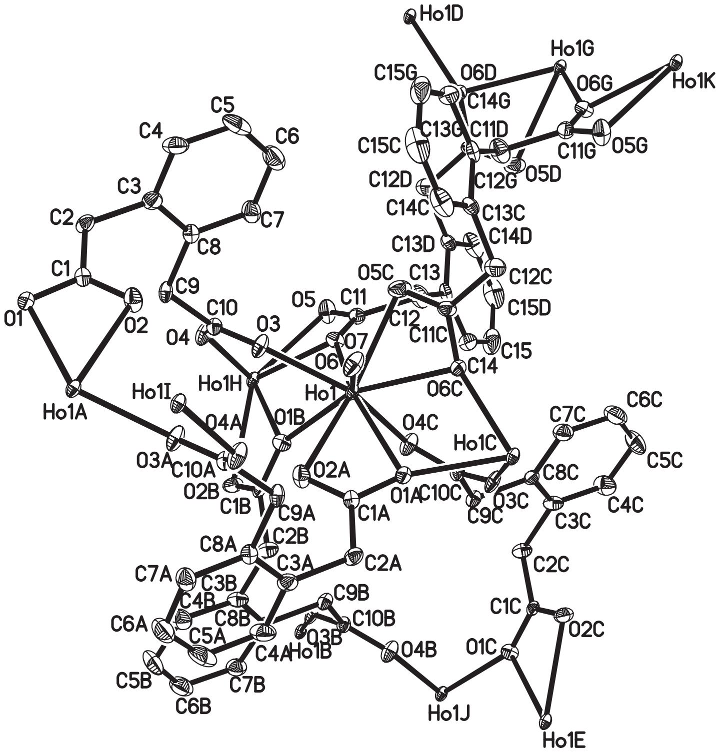

Figure 6. Coordination environment of Ho^{3+} and coordination modes of 1,2-pda ligands in **2** with 30% probability displacement ellipsoids. All hydrogen atoms and uncoordinated water are omitted for clarity.

3.3. *Luminescence properties*

The solid sample of **1** emits intense green fluorescence under ultraviolet light. The luminescence properties of **1** are similar to other terbium carboxylate complexes, with characteristic $^5D_4 \rightarrow {}^7F_j$ ($j = 6$–3) transition of Tb^{3+} ion and the positions of their emission bands are similar. Figure 7 gives the emission spectrum of **1** under excitation at 320 nm. The four emission bands are at 489 nm, 544 nm, 585 nm, and 619 nm, corresponding to the characteristic emission from $^5D_4 \rightarrow {}^7F_6$, $^5D_4 \rightarrow {}^7F_5$, $^5D_4 \rightarrow {}^7F_4$, and $^5D_4 \rightarrow {}^7F_3$ transitions of Tb^{3+} ion, respectively. Among them, the $^5D_4 \rightarrow {}^7F_5$ transition exhibits the strongest green emission.

Supplementary data

CCDC-635048 for **1** and 635081 for **2** contain the supplementary crystallographic data for this article. This data can be obtained free of charge from CCDC, 12 Union Road, Cambridge, CB2 1EZ, UK; Fax: +44(0)1223336033; Email: deposit@ccdc.cam.ac.uk.

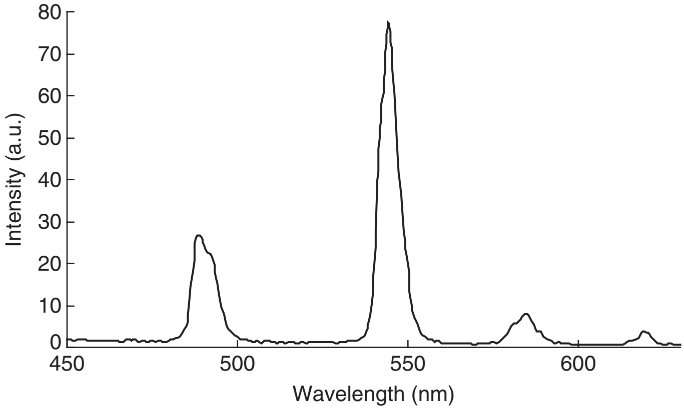

Figure 7. The emission spectrum for **1**, λex = 320 nm.

Acknowledgements

We are grateful to the Natural Science Foundation of Beijing (No. 2073022), the Science and Technology Program, the Beijing Municipal Education Commission (KM200510028007), and the Young Mainstay Teachers Foundation of Beijing Municipal Universities.

References

[1] P.J. Hagraman, D. Hagrman, J. Zubieta. *Angew. Chem., Int. Ed.*, **38**, 2638 (1999).
[2] M. Eddaoudi, J. Kim, M. O'Keeffe, O.M. Yaghi. *J. Am. Chem. Soc.*, **124**, 376 (2002).
[3] I. Kumagai, M. Akita-Tanaka, K. Inoue, M. Kurmoo. *J. Mater. Chem.*, **11**, 2146 (2001).
[4] C. Reinhard, H.U. Güdel. *Inorg. Chem.*, **41**, 1048 (2002).
[5] T.M. Reineke, M. Eddaoudi, M. Fehr, D. Kelley, O.M. Yaghi. *J. Am. Chem. Soc.*, **121**, 1651 (1999).
[6] C.G. Zheng, J. Zhang, Z.F. Chen, Z.J. Guo, R.G. Xiong, X.Z. You. *J. Coord. Chem.*, **55**, 835 (2002).
[7] Y.H. Wan, L.P. Jin, K.Z. Wang, L.P. Zhang, X.J. Zheng, S.Z. Lu. *New J. Chem.*, **26**, 1590 (2002).
[8] C. Daiquebonne, N. Kerbellec, K. Bernot, Y. Gérault, A. Deluzet, O. Guillou. *Inorg. Chem.*, **45**, 5399 (2006).
[9] X.J. Zheng, T.T. Zheng, L.P. Jin. *J. Mol. Struct.*, **740**, 31 (2005).
[10] Y.H. Wan, L.P. Zhang, L.P. Jin, S. Gao, S.Z. Lu. *Inorg. Chem.*, **42**, 4985 (2003).
[11] Y.F. Zhou, R.H. Wang, B.L. Wu, R. Cao, M.C. Hong. *J. Mol. Struct.*, **697**, 73 (2004).
[12] J.E.V. Babb, A.D. Burrows, R.W. Harrington, M.F. Mahon. *Polyhedron*, **22**, 673 (2003).
[13] L. Pan, K.M. Adams, H.E. Hernandez, X.T. Wang, C. Zheng, Y. Hattori, K. Kaneko. *J. Am. Chem. Soc.*, **125**, 3062 (2003).
[14] Y.Q. Xu, B.Q. Chen, Y.Q. Gong, D.Q. Yuan, F.L. Jiang, M.C. Hong. *J. Mol. Struct.*, **789**, 220 (2006).
[15] G.M. Sheldrick. Phase Annealing in SHELX-97: Direct Methods for Larger Structures; *Acta Cryst.*, **A46**, 467 (1990).
[16] G.M. Sheldrick. *SHELXL97, Program for X-ray Crystal Structure Solution*, University of Göttingen, Germany (1997).